Ab initio calculations of structural and dynamical properties of poly(*p*-phenylene) and poly(*p*-phenylene vinylene)

R. B. Capaz
Instituto de Física, Universidade Federal do Rio de Janeiro, Caixa Postal 68528, Rio de Janeiro, RJ 21941-972, Brazil

M. J. Caldas
Instituto de Física, Universidade de São Paulo, Caixa Postal 66318, São Paulo, SP 05389-970, Brazil
(Received 14 January 2002; revised 11 November 2002; published 9 May 2003)

We perform *ab initio* calculations within the local density approximation for infinite, isolated chains of poly(*para*-phenylene) (PPP) and poly(*para*-phenylene-vinylene) (PPV). Phonon frequencies at $\vec{k}=\vec{0}$ and structural properties are investigated with special focus on the ring-torsion barriers. Our results for PPV indicate a planar geometry, while for PPP we find a ring-torsion potential that is not affected by next-nearest-neighbor rings. This suggests the existence of a multiply degenerate ground state for PPP, with chiral, ordered, or random angle-alternating configurations having the same energy. In addition, we couple these results to a simple molecular-dynamics simulation in order to investigate the finite temperature behavior of the systems.

DOI: 10.1103/PhysRevB.67.205205 PACS number(s): 71.20.Rv, 82.35.Cd, 36.20.Ey

I. INTRODUCTION

Organic conjugated polymers form the basis of new electronic and optoelectronic devices, and as such have received a great deal of attention, both from the experimental and theoretical sides.[1] Among the most promising materials for light-emitting devices are the phenylene polymers poly(*para*-phenylene) (PPP) and poly(*para*-phenylene-vinylene) (PPV), ring-structured polymers with optical activity in the blue region, and that can be synthetized in the ''pure'' state or with a variety of substitutions (side chains appended to one or more of the phenylene *ortho*-carbon atoms, or even, for PPV, to the vinylene carbon atoms). In polymer-based light-emitting devices, the organic films form the active layers, usually between a metal and a transparent oxide electrode[1] and it is of prime interest to identify factors influencing carrier mobility and electron-hole recombination properties. Contrary to the extremely ordered arrangement of conventional semiconductor nanodevices, organic layers formed from long-chained polymers present intrinsic disordered regions in which the crystalline or almost-crystalline domains are immersed. The precise internal arrangement of the crystalline regions is extremely dependent on the specific substitution employed;[2] however, we may suppose that the effective mobility of carriers is dominated by disordered regions, where it is very probable that interchain interactions can be neglected. In this way, information on the properties of isolated chains is needed and can be very useful for modeling the material. In fact, it is well known that the interesting electrical properties of these compounds come from the large conjugation and π-electron delocalization along the chain length. These characteristics are strongly affected by torsion angles between rings: Increase in the torsion angles decreases conjugation and mobility (increasing the effective mass) and increases the gap energy. On the other hand, it is believed that charge carriers in polymers, electrons or holes, are ''dressed'' by backbone distortion (polarons[3]); thus on-chain mobility should also be strongly influenced by the phonon structure.

We present in this work a study of infinite, isolated PPP and PPV chains, focusing on structural, vibrational, and dynamical properties. We start from *ab initio* calculations for ground-state structural properties, torsion barriers, and phonon spectra. We then couple our *ab initio* results to a simple molecular-dynamics scheme, specifically designed to address torsional configurations, in order to investigate the dynamical behavior of the systems. We briefly present in the next section the calculational details for the *ab initio* method used, and then in Secs. III and IV we discuss our ground-state results. The finite-temperature behavior is discussed in Sec. V.

We show that, as expected, ring-torsion modes are very soft compared to bond bending or stretching, and that torsion angles are virtually independent of the second-ring neighborhood. As a result, we find that finite-temperature behavior is dominated by ring libration for both polymers.

II. METHOD

Our calculations are based on local-density-functional theory,[4,5] with the Ceperley-Alder[6] exchange correlation as parametrized by Perdew and Zunger.[7] We adopt the supercell approximation, which consists of embedding the system on a sufficiently large unit cell periodically repeated in all three dimensions. When calculating properties of isolated molecules or polymers, this implies that a large enough ''vacuum region'' has to be included in order to avoid spurious interactions between the molecules and their periodic images. A vacuum region of typically 8–10 Å in all directions is enough to provide a good isolation for molecules. We use orthorhombic supercells with dimensions 15 Å$\times$12 Å$\times c$ for both PPP and PPV. The cell dimension along the chain axis is the lattice constant c, which is adjusted in order to minimize total energy. The unit cells contain two (single-cell) or four (double-cell) phenyl rings for PPP and one (single-cell) or two (double-cell) phenyl rings for PPV, depending on the specific calculation. Calculations are done with a two-$\vec{k}$-point sampling [$(0,0,\frac{1}{8})$ and $(0,0,\frac{3}{8})$ in units of

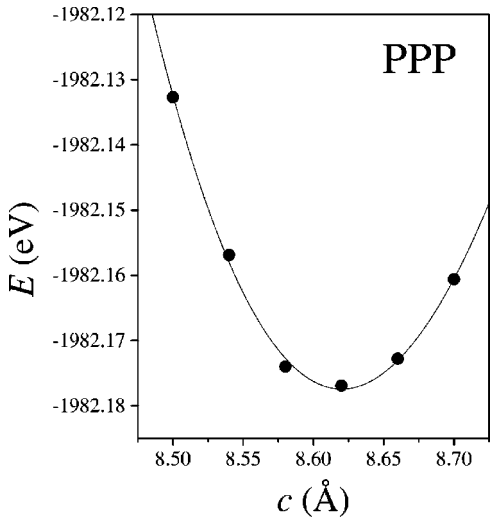

FIG. 1. Total energy vs lattice constant for PPP. The full line is a third-order polynomial fit.

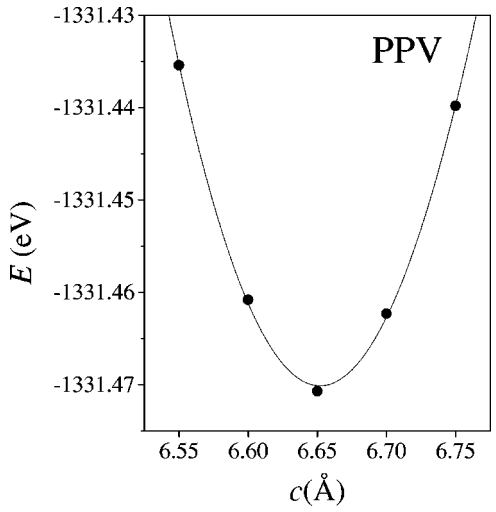

FIG. 2. Total energy vs lattice constant for PPV. The full line is a third-order polynomial fit.

$2\pi/c$] for single-cell PPP and PPV. Double-cell PPV and PPP are sampled at $(0,0,\frac{1}{4})$ only, which unfolds exactly into the two previous $\vec{k}$ points for the single-cell structures. Going from two to one $\vec{k}$ points for single-cell PPV changes the lattice constant by less than 0.5%.

We use *ab initio* pseudopotentials with optimized plane-wave convergence.[8] This is especially important when dealing with first-row atoms such as carbon, which naturally requires a large plane-wave basis to describe its localized $2p$ states. Employing optimized pseudopotentials allows the use of a cutoff energy of $E_c = 40$ Ry. This corresponds to 45 000, 90 000, 35 000, and 70 000 plane waves for single-cell PPP, double-cell PPP, single-cell PPV, and double-cell PPV, respectively. Increasing the cutoff to 60 Ry for PPV changes the ground-state energy by only 0.046 eV/atom and the lattice constant by only 0.05%. The self-consistent Kohn-Sham equations are solved iteratively by direct minimization of the energy functional using a preconditioned conjugate gradient scheme.[9]

III. GROUND-STATE GEOMETRY AND ELASTIC PROPERTIES

Minimum-energy atomic configurations for PPP and PPV are obtained by relaxation of all atomic coordinates until Hellman-Feynman forces are below 0.05 eV/Å for each value of the lattice constant. The equilibrium lattice constants (c_0) are then given by the minimum in the energy vs c plots, shown in Fig. 1 for PPP and Fig. 2 for PPV. We find $c_0 = 8.62$ Å for PPP and $c_0 = 6.65$ Å for PPV, to be compared with the experimental values of 8.54 Å (Refs. 10–12) and 6.54 Å (Ref. 13). The 1%–2% difference is typical of local-density approximation (LDA) calculations. From the second derivative at equilibrium one can calculate Young's modulus Y as

$$Y = \frac{c_0}{A}\left.\frac{d^2E}{dc^2}\right|_{c_0}, \qquad (1)$$

where A is the cross-sectional area. Using experimentally determined values for A in crystalline material in the usual herringbone structure ($A_{\mathrm{PPP}} = 21.47$ Å^2 and $A_{\mathrm{PPV}} = 20.47$ Å^2),[10–12] we obtain $Y = 364$ GPa for PPP and $Y = 325$ GPa for PPV. To the best of our knowledge, Young's moduli have not been experimentally determined yet for either PPP or PPV. Our calculated results are not much different from either theoretical[14] (389 GPa) or experimental[15] (373 GPa) results for *trans*-polyacetylene (TPA). The larger Y values for TPA are due to a smaller cross-sectional area ($A_{\mathrm{TPA}} = 15.52$ Å^2).[16] A more meaningful quantity for comparing effective monomer force constants along the chain is the product YA. For this quantity, we have $(YA)_{\mathrm{PPP}} > (YA)_{\mathrm{PPV}} > (YA)_{\mathrm{TPA}}$, thus indicating that the presence of vinylene segments makes conjugated chains softer.

Atomic arrangements for monomer units of PPP and PPV are shown schematically in Fig. 3. Calculated bond lengths and bond angles, along with available experimental results, are presented in Table I for PPP and Table II for PPV. Values for PPP are slightly different from our previously reported ones[17] due to the different k-point sampling used. Both structures present a slightly quinoid configuration, an effect which is more pronounced in PPV. Calculated values for bond lengths and angles are in excellent agreement with available experimental data.

Due to a compromise between chain conjugation (which tends to make the molecule planar) and steric repulsions between orthohydrogens (which tends to do the opposite), adjacent phenyl rings in PPP are tilted with respect to each other by a torsion angle θ (in an alternate pattern for the primitive unit cell). Crystalline packing is also expected to reduce this torsion angle, which is an important structural parameter, not only because it reveals the strength of chain conjugation and crystalline packing, but also because it can strongly influence optical parameters such as the band gap.[18] Our calculations give $\theta = 27.2°$.[19] Interestingly, hydrogen atoms arrange themselves in planes that are slightly out of their respective carbon ring planes. Torsion angles between adjacent hydrogen planes are thus slightly larger, 28.3°.

TABLE I. Bond distances (in Å) and bond angles (in degrees) for PPP. Atom labels follow the notation of Fig. 3. Experimental results (Refs. 44–46) refer to central rings in the following molecular crystals: Terphenyl (x-ray and neutron diffraction) (Refs. 44,46) and quaterphenyl (x-ray diffraction) (Ref. 45).

Parameter	This work	Ref. 44	Ref. 45	Ref. 46
Bond length				
C_1–C_2	1.405	1.377	1.403–1.409	1.395–1.425
C_2–C_4	1.389	1.407	1.397–1.409	1.356–1.406
C_6–C_7	1.469	1.496	1.502	1.469–1.505
C–H	1.103	1.09	0.96–1.08	1.110–1.129
Bond angle				
C_2–C_1–C_3	117.8	116.9	117.1	115.0–118.3
C_1–C_2–C_4	121.1	121.5	121.3–121.7	120.6–123.1
C_1–C_3–H	119.2	124–126	116.0–119.4	117.7–119.7
θ	27.2			

There are no experimental values for the torsion angle of isolated PPP chains, but our calculated value fits well between measured values for crystalline quaterphenyl[20] (22.7°) and gaseous biphenyl[21,22] (44.4°). As expected, quaterphenyl in a crystalline environment has a smaller torsion angle due to packing effects, and gaseous biphenyl has a larger torsion angle since each ring has only one neighbor (instead of two for the longer chains); therefore the conjugation driving force for planarity is smaller. Our results are also in good agreement with previous LDA calculations for PPP[18] (27.4°). A larger torsion angle (37.8°) was obtained from semiempirical Hartree-Fock calculations in isolated quaterphenyl.[23]

In the case of PPV, calculations for the single-ring unit cell suggest a planar configuration for the ground state. Planarity of PPV is consistent with its larger quinoid character (compared to PPP), with the fact that only two hydrogens per phenyl ring actually participate strongly in steric repulsion interactions (with vinylene hydrogens) as opposed to four in PPP, and with the existence of an extra degree of freedom (namely the opening of the zigzag angle at the vinyl segment) to avoid loss of planarity while still minimizing steric repulsions. Indeed, our calculated zigzag angle (C_6-C_7-C_8 in

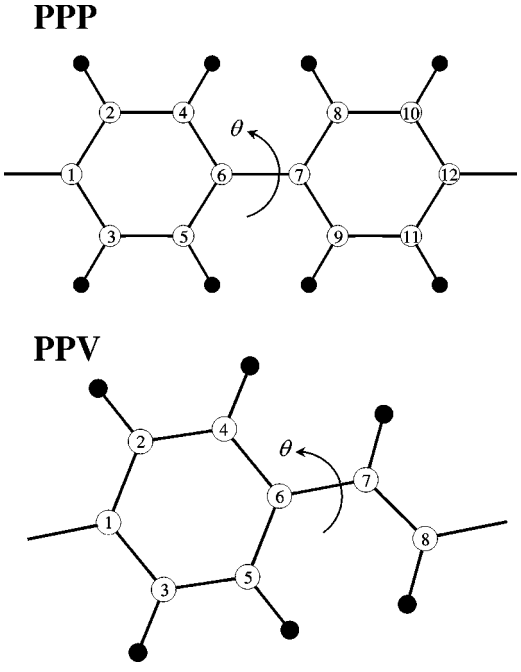

FIG. 3. Atomic configuration for PPP and PPV monomers, labeled to help in reading the tables. Carbon and hydrogen atoms are in open and solid circles, respectively. The torsion angle θ is defined as the angle between adjacent phenyl rings for PPP and between a ring and the chain backbone for PPV.

TABLE II. Bond distances (in Å) and bond angles (in degreees) for PPV. Atom labels follow the notation of Fig. 3. Experimental results refer to x-ray diffraction studies on stilbene molecular crystals (Ref. 48).

Parameter	This work	Ref. 48
Bond length		
C_1–C_2	1.411	1.397
C_2–C_4	1.383	1.387
C_1–C_3	1.414	1.394
C_6–C_7	1.443	1.469
C_7–C_8	1.361	1.318
C_2–H	1.103	0.93
C_3–H	1.104	1.02
C_7–H	1.108	1.00
Bond angle		
C_2–C_1–C_3	117.3	117.8
C_1–C_2–C_4	121.1	121.4
C_1–C_3–C_5	121.6	120.6
C_6–C_7–C_8	126.3	126.7
C_1–C_2–H	119.4	117.2
C_1–C_3–H	118.7	119.0
C_6–C_7–H	115.0	116.1

Fig. 3) is 126.3°, considerably larger than 120° and only slightly smaller than the 128° suggested for stilbene.[24]

Planarity of PPV is in discrepancy with x-ray diffraction[24] in crystalline samples, which suggests a nonzero torsion angle between the phenyl rings and the vinyl segment. Experimental torsion angles are found to increase with temperature from 8° at 20 °C to 13° at 400 °C and adjacent phenyl rings are observed to rotate in an alternate fashion.[24] To investigate this geometrical configuration we have performed calculations with a double unit cell. It is extremely difficult to determine the exact value of the torsion angle (if any) since, as will shall see in the next section, ring-torsion modes in PPV are very soft and therefore differences in total energy between planar and nonplanar (with a small angle) configurations are exceedingly small. For instance, we find the energy difference between planar PPV and a chain with a torsion angle of 7° to be less than 1 meV per cell. Our results indicate, nonetheless, a planar configuration for the isolated PPV chain. It is to be remarked, however, that Raman spectroscopy[25] results suggest a more complicated symmetry-breaking distortion where the vinyl segment is itself nonplanar, so that the torsion angle between rings results not solely from the phenylene-vinylene torsion, but from a continuous torsion along the monomer. We recall that in crystalline PPV in the herringbone structure, vinylene segments of one chain are packed close to the phenylene units of neighboring chains. The experimentally observed deviation from planarity could thus be a symmetry-breaking effect due to interchain interactions in the crystalline environment, absent for the isolated chain; it is, however, very likely that this continuous torsion would be difficult to reproduce theoretically even for the packed chains. A similar difficulty was found for the small related molecules styrene and stilbene, where nonplanarity was predicted by theory[26] but is not seen by experiments in solution, probably, as discussed by the authors, because it is ''averaged out.'' Indeed, due to the extreme softness of these torsion modes, any theoretical prediction for the exact value of the torsion angle, including ours, should be taken as an estimate.

IV. VIBRATIONAL PROPERTIES

Vibrational spectra of both PPP[27–32] and PPV[25,33–38] have been studied both theoretically and experimentally. We calculate vibrational normal-mode frequencies and displacements by directly evaluating the matrix of force constants using a finite-difference technique for single-cell systems (two phenylene rings for PPP, one phenylene-vinylene unit for PPV).

Table III shows our calculated vibrational frequencies at $\vec{k}=\vec{0}$ (Γ) for PPP, along with previously published results. In order to facilitate comparison, we adopt the symmetry labeling of Ref. 29, based on the D_{2h} point group of single-ring, planar PPP. Since our ground-state structure is nonplanar with two rings per unit cell, modes at the boundary (Z) of the single-ring Brillouin zone are folded into our Γ point; therefore we have twice as many modes at Γ. The overall agreement between calculated and experimental frequencies is rather good, considering that these are calculated modes for the isolated chains and experiments are usually done in the crystalline phase. It is also important to emphasize that, contrary to all previous theoretical works, our calculation has no fitting parameters and the frequencies are not scaled by any *ad hoc* factor. The higher frequency modes ($\sim 3000\ \mathrm{cm}^{-1}$) correspond to the C-H stretch. For the remaining modes, as a general trend, in-plane modes are higher in frequency than out-of-plane ones, since they necessarily involve bond-length and bond-angle variations.[39]

Table IV shows our calculated vibrational frequencies at Γ for PPV, along with previously published results. We adopt the symmetry labeling of Ref. 36 based on the C_{2h} point group. As a general remark, the ring C-C stretch frequencies group around 1274–1546 cm^{-1}, while we find the vinylene stretch frequency at 1635 cm^{-1}, close to the value for the phonon replica extracted from experimental data[2] on the PPV luminescence band (note that a redshift is expected for photoinduced modes[35]). Similarly to PPP, the higher-frequency modes ($\sim 3000\ \mathrm{cm}^{-1}$) correspond to the C-H stretch and out-of-plane degrees of freedom (such as torsion-angle variations) are generally softer than in-plane ones.

For both polymers, the softness of out-of-plane modes suggests variations in torsion angles to be the dominant dynamical behavior at low temperatures. As mentioned before, torsion-angle variations can affect dramatically the electronic and optical properties of these materials.[18] For these reasons, we study them in more detail in the next section.

V. TORSION POTENTIALS, DEFECTS, AND FINITE-TEMPERATURE BEHAVIOR

Polyphenyls present an extremely rich finite-temperature behavior: ring librations and flips,[40] order-disorder phase transitions,[20] and ring-torsion defects similar to those in polyaniline.[41] A key ingredient to the understanding of these effects is the analysis of torsion potentials. Accordingly, we performed calculations of the torsion potentials for both PPP

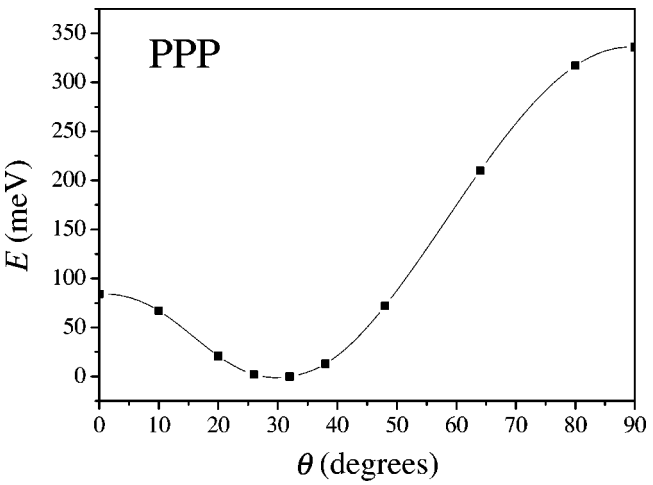

FIG. 4. Total energy per unit cell as a function of the torsion angle θ for PPP. The ground-state energy is set to zero. The inter-ring torsion potential is obtained by dividing the total energy by 2, since PPP has two rings per unit cell. The line is a spline fit to the calculated data points (squares).

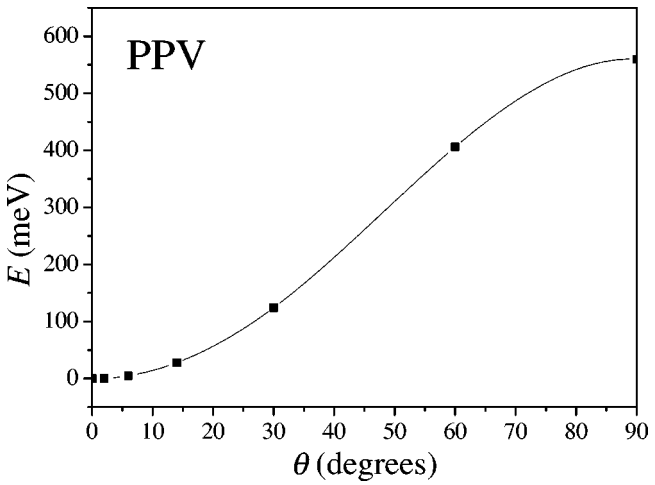

FIG. 5. Total energy per unit cell as a function of the torsion angle θ (equivalent to the interring torsion potential) for PPV. The ground-state energy is set to zero. The line is a spline fit to the calculated data points (squares).

and PPV. They are constrained total-energy calculations, on which the torsion angle θ is kept fixed at different values while all other coordinates are allowed to relax at fixed lattice constant c_0. These calculations allow us to estimate the energy barriers for thermally induced ring flips over angular maxima in the potential. The resulting potentials are shown in Fig. 4 for PPP and Fig. 5 for PPV.

As already mentioned, by keeping the vinyl segment planar, we find a single potential minimum at $\theta=0°$ for PPV (planar configuration). Crystalline packing will probably affect both the minimum energy configuration and the torsion potential barriers: While it might produce a nonzero equilibrium torsion angle, it will certainly enhance the barrier for ring flips over 90°. Complete rotation of phenyl rings in crystalline PPV has been measured by NMR with an activation energy of 651 meV.[42] Our barrier of 560 meV, directly estimated from the torsion potential in Fig. 5 is, as expected, smaller due to the absence of packing effects.

PPP is nonplanar, and there are two energy barriers at $\theta=0°$ and $\theta=90°$. These are, respectively, 84 meV and 336 meV per unit cell. Since each unit cell contains two phenyl-phenyl angles, the activation energies *per angle* are 42 meV and 168 meV, respectively. X-ray[40] and nuclear magnetic resonance[43] (NMR) measurements of activation energies per angle for ring flips over $\theta=0°$ are 23.7 meV (x ray) and 22.8 meV (NMR) for *p*-terphenyl and 27.3 meV (x-ray) and 26.8 meV (NMR) for *p*-quaterphenyl. The experimental results refer to very short oligomers, in which any ring is always in a nearest-neighbor position to at least one chain end, thus facilitating the flip (leading to a lower-energy barrier). We may say that our value is very probably representative for the infinite isolated chain.

We can go beyond the ''adiabatic'' analysis based on the torsion potential to study dynamical effects associated with ring libration. As we saw in the preceding section, we may decouple out-of-plane ''rotational'' modes from the other vibrational modes: This approximation is justified by the difference in strength between in-plane and out-of-plane force constants, the latter being considerably softer and therefore expected to dominate chain dynamics at low temperatures. Dynamical chain behavior can then be investigated by ''angular dynamics'' simulations of the motion of the phenyl

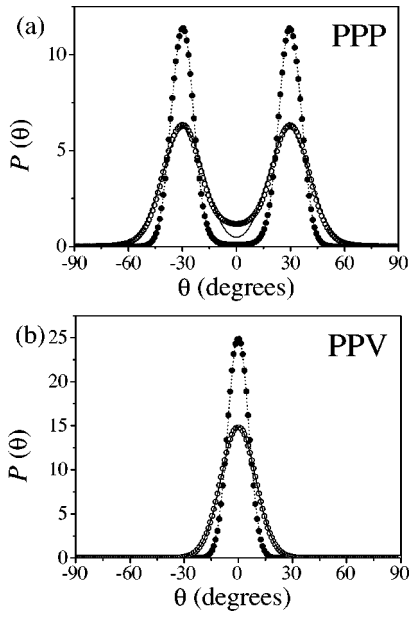

FIG. 6. Probability distribution functions $P(\theta)$ for torsion angles for (a) PPP and (b) PPV. Solid circles and dashed lines represent $T=100$ K, whereas open circles and full lines represent $T=300$ K. Lines are Gaussian fits.

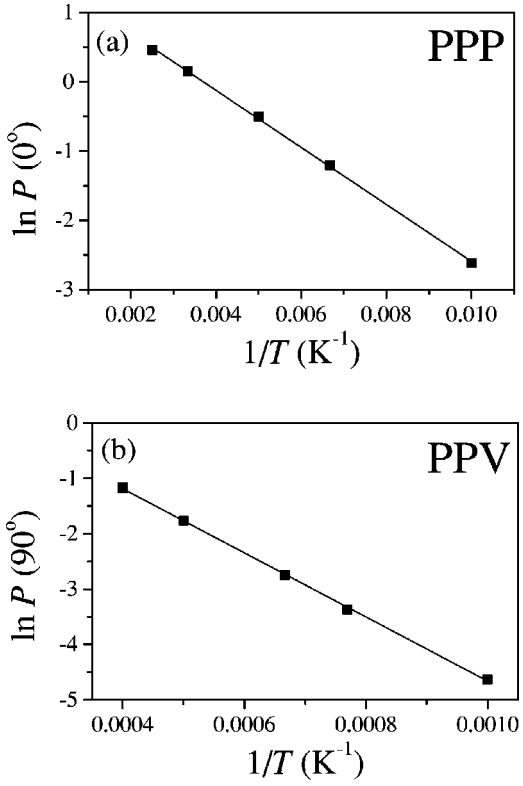

FIG. 7. Arrhenius plots for ring flips (a) over $\theta=0°$ for PPP and (b) over $\theta=90°$ for PPV.

TABLE III. Phonon frequencies (in cm^{-1}) at Γ for PPP, along with other calculated (Refs. 27 and 29) and experimental (Refs. 30–32) results. For mode description, op refers to out-of-plane modes, ip to in-plane modes, and $\Gamma(Z)$ to modes at the single-ring Brillouin zone center (edge).

			Theory		Experiment		
Symmetry	Description	This work	Ref. 27	Ref. 29	Ref. 30	Ref. 31	Ref. 32
B_{2g}	op, Z	39					
B_{3u}	op, Z	144					
B_{3g}	ip, Z	168					
B_{1g}	op, Z	230					
B_{2u}	ip, Z	285					
B_{2g}	op, Γ	374	402	410			409
A_u	op, Γ	475	401	367			
A_u	op, Z	475					
B_{3u}	op, Γ	495	458	457			
B_{3g}	ip, Γ	501	460	488			
B_{1u}	ip, Z	578					
A_g	ip, Z	593					
B_{3u}	op, Z	652					
B_{3g}	ip, Γ	653	602	625			623
B_{3g}	ip, Z	674					
B_{2g}	op, Z	702					
B_{2g}	op, Γ	770	760	754			
A_g	ip, Γ	809	846	792		805	796
B_{1g}	op, Γ	859	834	823			
B_{1g}	op, Z	860					
B_{3u}	op, Γ	873	790	797	804		
A_u	op, Z	880					
A_u	op, Γ	882	961	951			
B_{3u}	op, Z	888					
B_{2g}	op, Z	899					
B_{2g}	op, Γ	901	945	968			999
B_{1u}	ip, Γ	979	968	984	998		
B_{1u}	ip, Z	986					
B_{1u}	ip, Γ	1045	1051	1045			
A_g	ip, Z	1049					
B_{2u}	ip, Γ	1094	1075	1162			
B_{2u}	ip, Z	1112					
A_g	ip, Γ	1123	1127	1233		1220	1223
A_g	ip, Z	1146					
B_{3g}	ip, Z	1235					
B_{1u}	ip, Z	1249					
B_{3g}	ip, Γ	1270	1328	1325			
B_{2u}	ip, Γ	1296	1268	1275			
A_g	ip, Γ	1319	1289	1282		1280	1281
B_{2u}	ip, Z	1369					
B_{1u}	ip, Γ	1445	1510	1487	1482		
B_{2u}	ip, Γ	1453	1440	1399	1400		
B_{2u}	ip, Z	1462					
B_{1u}	ip, Z	1506					
B_{3g}	ip, Z	1522					
B_{3g}	ip, Γ	1568	1654	1601			
A_g	ip, Γ	1617	1661	1626		1595	1593
A_g	ip, Z	1641					

TABLE III. (*Continued*).

			Theory		Experiment		
Symmetry	Description	This work	Ref. 27	Ref. 29	Ref. 30	Ref. 31	Ref. 32
B_{3g}	ip, Z	3038					
B_{3g}	ip, Γ	3038					
B_{1u}	ip, Γ	3040					
B_{1u}	ip, Z	3040					
B_{2u}	ip, Γ	3051					
B_{2u}	ip, Z	3051					
A_g	ip, Γ	3054					
A_g	ip, Z	3054					

rings. In these simulations, all degrees of freedom are frozen except for the ring angles, whose trajectories $\theta(t)$ are obtained by numerical integration of their assumed classical equations of motion. The torque on each ring is obtained from their instantaneous configuration via the interring torsion potential calculated above. We have performed simulations on chains containing 100 rings with periodic boundary conditions, using a Verlet algorithm with a time step of 10^{-15} s.

In Fig. 6(b) we show torsion angle probability distributions, $P(\theta)$, for 100 K and 300 K for PPV. Notice that the distributions are Gaussian functions centered in $\theta=0°$. Analysis of the Gaussian widths for different temperatures shows root-mean-square librations of the torsion angles to be proportional to $T^{1/2}$, with a coefficient of 0.56 deg/K$^{1/2}$. These dynamical simulations also allow us to obtain the frequency of ring flips over $\theta=90°$, which is essentially proportional to $P(90°)$. Therefore, an Arrhenius-plot analysis of $\ln P(90°)$ vs $1/T$ [Fig. 7(b)] gives the activation energy for 180° rotation of phenyl rings in PPV. The straight line is a clear signature of a thermally activated process with a calculated activation energy of 499 meV, close to our calculated adiabatic value of 560 meV.

Figure 6(a) shows the probability distribution of torsion angles for PPP, also for 100 K and 300 K. Note the expected double-peak structure, with essentially temperature-independent peak positions, showing that the dominant low-temperature behavior of the phenyl rings in PPP is a small-angle libration around the equilibrium values. The solid and dashed lines are best fits to two Gaussian functions. Two Gaussians fit well the distribution at 100 K over the whole range of angles, but this is not the case for the distribution at 300 K in the vicinity of $\theta=0°$. From the Gaussian fit at different temperatures, we obtain a root-mean-square libration amplitude σ, which is essentially proportional to $T^{1/2}$, with a proportionality coefficient of 0.66 deg/K$^{1/2}$. Similarly to the case of PPV, we can obtain the activation energy for ring flips over $\theta=0°$ from the Arrhenius plot in Fig. 7(a). The calculated value is 35 meV, close to the adiabatic value of 42 meV.

In the analysis above, the interring potential was obtained from the total energy results by assuming that rings interact only with their nearest-neighbor rings and longer-range interactions are unimportant. We can test this hypothesis by performing total-energy calculations on supercells with four rings and by comparing the total energies of two distinct configurations: $(-\theta/2,\theta/2,-\theta/2,\theta/2)$ and $(-\theta/2,\theta/2,3\,\theta/2,\theta/2)$. Notice that in both configurations the nearest-neighbor torsion angle is the same (except for sign), but one of the second-nearest-neighbor torsion angles is different. If second-nearest-neighbor interactions were revelant, we would obtain different values for the total energy of these two configurations. We find that total-energy differences between the two configurations are less than 5 meV for the whole range of θ, confirming that second and more distant neighbors ring interactions can be safely neglected. This is in good accord with the results of Cuff and Kertesz,[29] who find a strong similarity of the vibrational frequencies in helical or alternate terphenyl conformers, also as a consequence of this weak coupling between second-nearest-neighbor rings.

This result has some important consequences. First of all, it implies that an infinite and isolated PPP chain has a multiply degenerate ground state: Essentially any chain configuration for which the torsion angle between two adjacent rings has an absolute value of $\theta=27.2°$ is a valid ground state. This includes, for instance, chains with an spiral or even disordered configuration of torsion angles and chains containing localized ''defects'' in the ring-alternation pattern. Some of these defects could connect two domains of different ground states, very much like a soliton in *trans*-polyacetylene, for instance. Our results imply that this ring-torsion soliton has essentially zero formation energy and therefore they are abundant at *any* temperature in the isolated chain. Of course, this behavior can be affected in crystalline samples by interchain interactions, but nevertheless it is an interesting and somewhat unexpected result. It can also lead to an increased difficulty in obtaining ordered samples from PPP as compared to planar PPV. Another implication of this result concerns coupling to light. As already mentioned, the single-particle gap energy for ring-structured polymers increases with torsion angle;[18] furthermore, the exciton binding energy depends on the ''conjugation length'' or ''exciton length.'' The more disordered structure of PPP could lead to a broader distribution of exciton lengths and energies, consistent with the very wide exciton line shape of PPP as compared to PPV.

TABLE IV. Phonon frequencies (in cm^{-1}) at Γ for PPV, along with other calculated and experimental results. For mode description, op refers to out-of-plane modes and ip to in-plane modes. The table also shows a few unidentified experimental modes.

			Theory			Experiment				
Symmetry	Description	This work	Ref. 33	Ref. 36	Ref. 37	Ref. 37	Ref. 36	Ref. 47	Ref. 25	Ref. 3
B_g	op	147								
A_u	op	220								
A_g	ip	310		328.1	311	327				
B_g	op	327								
A_u	op	390								
B_u	ip	430		431.2	425	428	429	429	430	
A_u	op	532	522					555	556	
A_g	ip	622		619.9	603	634				
A_g	ip	659		692.3	660	662				
B_g	op	696								
B_g	op	785								
B_u	ip	799		771.5	787	784	785	784	784	
A_u	op	818	814					837	838	
B_g	op	853								
A_g	ip	899		968.2	896	887	966		963	
A_u	op	911								
B_g	op	926								
A_u	op	930	1005					965	966	
B_u	ip	978	1135	1012.6	1026	1013	1013	1013	1014	
B_u	ip	1076			1117	1107		1108	1107	
				1169.9			1178	1176	1180	
A_g	ip	1111	1181	1174.3	1163	1170	1174		1172	1170
A_g	ip	1185			1192	1197				1197
				1282.0						
B_u	ip	1187			1181	1179		1176	1194	
				1205.0		1210	1211	1210	1211	
A_g	ip	1262		1303.5	1295	1301	1304		1301	1301
B_u	ip	1268		1269.3	1269	1271	1271	1267	1271	
A_g	ip	1274	1272	1330.1	1330	1329	1327		1329	1327
						1302			1302	
B_u	ip	1367		1341.1	1333	1340	1339	1336	1340	
B_u	ip	1458		1416.7	1436	1424	1424	1423	1424	
B_u	ip	1485	1543	1528.4	1516	1518	1518	1519	1519	
									1415	
A_g	ip	1493	1600	1549.6	1538	1546	1550		1547	1546
A_g	ip	1546	1616	1586.7	1587	1582	1586		1582	1582
A_g	ip	1635	1659	1629.2	1636	1625	1628		1626	1625
A_g	ip	2951								
B_u	ip	2975		3027.9				3024		
A_g	ip	3058								
B_u	ip	3064		3065.9				3076		
A_g	ip	3116								
B_u	ip	3125		3125.1				3105		

As a last remark, we note that ring-torsion structure and dynamics are bound to depend strongly on the chain chemical structure, that is, we expect the conformation and barriers to depend on the specific substitutions appended on the chain. The results presented here apply only to the pure polymers.

VI. SUMMARY AND CONCLUSIONS

We performed *ab initio* calculations for the structural properties of isolated PPP and PPV chains, from which we extract the phonon spectra and ring-torsion angles and barriers. Our results indicate a planar configuration for isolated

PPV chains, while for isolated PPP chains rings are twisted with respect to neighbors by an angle of $\sim 27°$. We find, as expected, that out-of-plane modes (ring torsion) can be found at much lower energies when compared to bond-stretching or bond-bending modes. We assume that the soft ring-torsion modes dominate room-temperature behavior and investigate thus the dynamics of the system by performing molecular dynamics simulations for isolated, infinite chains. Our results for the activation energies for ring flips are in good agreement with experimental data. Moreover, we find that next-nearest-neighbor ring interactions can be neglected, leading to a multiply degenerate ground state with chiral and alternating torsion angle sequences having the same energy. Therefore we can conclude that torsion-alternation defects can exist at any temperature for an isolated PPP chain.

ACKNOWLEDGMENT

This work was partially supported by Brazilian funding agencies CNPq, FAPERJ, FAPESP, PRONEX-MCT, FUJB-UFRJ, and Instituto de Nanociências. The use of computational facilities at Núcleo de Atendimento em Computação de Alto Desempenho (NACAD-COPPE/UFRJ) is also acknowledged.

[1] R.H. Friend, R.W. Gymer, A.B. Holmes, J.H. Burroughes, R.N. Marks, C. Taliani, D.D.C. Bradley, D.A. dos Santos, J.L. Brédas, M. Logdlund, and W.R. Salaneck, Nature (London) **397**, 121 (1999).

[2] S.J. Martin, D.D.C. Bradley, P.A. Lane, H. Mellor, and P.L. Burn, Phys. Rev. B **59**, 15 133 (1999).

[3] M. Baïtoul, J. Wery, J.P. Buisson, G. Arbuckle, H. Shah, S. Lefrant, and M. Hamdoume, Polymer **41**, 6955 (2000).

[4] P. Hohenberg and W. Kohn, Phys. Rev. **136**, 864B (1964).

[5] W. Kohn and L.J. Sham, Phys. Rev. **140**, 1133A (1965).

[6] D.M. Ceperley and B.J. Alder, Phys. Rev. Lett. **45**, 566 (1980).

[7] J.P. Perdew and A. Zunger, Phys. Rev. B **23**, 5048 (1981).

[8] A.M. Rappe, K.M. Rabe, E. Kaxiras, and J.D. Joannopoulos, Phys. Rev. B **41**, 1227 (1990).

[9] M.C. Payne, M.P. Teter, D.C. Allan, T.A. Arias, and J.D. Joannopoulos, Rev. Mod. Phys. **64**, 1045 (1992).

[10] P. Kovacic, M.B. Feldman, J.P. Kovacic, and J.B. Lando, J. Appl. Polym. Sci. **12**, 1735 (1968).

[11] M. Stamm and J. Hocker, J. Phys. (Paris), Colloq. **44**, C3-667 (1983).

[12] M. Stamm, J. Fink, and B. Tieke, Mol. Cryst. Liq. Cryst. **118**, 281 (1985).

[13] D. Chen, M.J. Winokur, M.A. Masse, and F.E. Karasz, Phys. Rev. B **41**, 6759 (1990).

[14] D.E. Tuyarot, B. Koiller, and R.B. Capaz, Phys. Rev. B **61**, 7187 (2000).

[15] S.Y. Hong and M. Kertesz, Phys. Rev. B **41**, 11 368 (1990).

[16] C.R. Fincher, Jr., C.-E. Chen, A.J. Heeger, A.G. MacDiarmid, and J.B. Hastings, Phys. Rev. Lett. **48**, 100 (1982).

[17] R.B. Capaz and M.J. Caldas, J. Mol. Struct.: THEOCHEM **464**, 31 (1999).

[18] C. Ambrosch-Draxl, J.A. Majewski, P. Vogl, and G. Leising, Phys. Rev. B **51**, 9668 (1995).

[19] Since the torsion angle is an important structural parameter, we have tested its convergence with respect to a further increase in the $\vec{k}$-point sampling from 2 to 4$\vec{k}$-points in the irreducible Brillouin zone. We found no significant change.

[20] J.L. Baudour, Y. Delugeard, and P. Rivet, Acta Crystallogr., Sect. B: Struct. Crystallogr. Cryst. Chem. **34**, 625 (1978).

[21] A. Almenningen, O. Bastiansen, L. Fernholt, B.N. Cyvin, S.J. Cyvin, and S. Samdal, J. Mol. Struct. **128**, 59 (1985).

[22] O. Bastiansen and S. Samdal, J. Mol. Struct. **128**, 115 (1985).

[23] J.L. Brédas, B. Thémans, J.G. Fripiat, J.M. André, and R.R. Chance, Phys. Rev. B **29**, 6761 (1984).

[24] D. Chen, M.J. Winokur, M.A. Masse, and F.E. Karasz, Polymer **33**, 3116 (1992).

[25] A. Sakamoto, Y. Furukawa, and M. Tatsumi, J. Phys. Chem. **96**, 1490 (1992).

[26] C.H. Choi and M. Kertesz, J. Phys. Chem. A **101**, 3823 (1997).

[27] G. Zannoni and G. Zerbi, J. Chem. Phys. **82**, 31 (1985).

[28] L. Cuff, C. Cui, and M. Kertesz, J. Am. Chem. Soc. **116**, 9269 (1994).

[29] L. Cuff and M. Kertesz, Macromolecules **27**, 762 (1994).

[30] L.W. Shacklette, R.R. Chance, D.M. Ivory, G.G. Miller, and R.H. Baughman, Synth. Met. **1**, 307 (1979).

[31] Y. Pelous, G. Froyer, C. Herold, and S. Lefrant, Synth. Met. **29**, E17 (1989).

[32] Y. Furukawa, H. Ohta, A. Sakamoto, and M. Tasumi, Spectrochim. Acta, Part A **47**, 1367 (1991).

[33] D. Raković, R. Kostić, L.A. Gribov, and I.E. Davidova, Phys. Rev. B **41**, 10 744 (1990).

[34] W.Z. Wang, A. Saxena, and A.R. Bishop, Phys. Rev. B **50**, 6068 (1994).

[35] B. Tian, G. Zerbi, R. Schenk, and K. Müllen, J. Chem. Phys. **95**, 3191 (1991).

[36] B. Tian, G. Zerbi, and K. Müllen, J. Chem. Phys. **95**, 3198 (1991).

[37] I. Orion, J.P. Buisson, and S. Lefrant, Phys. Rev. B **57**, 7050 (1998).

[38] P. Papanek, J.E. Fischer, J.L. Sauvajol, A.J. Dianoux, G. Mao, M.J. Winokur, and F.E. Karasz, Phys. Rev. B **50**, 15 668 (1994).

[39] For a nonplanar chain, mode classification into ''in-plane'' and ''out-of-plane'' is of course only approximate.

[40] J.L. Baudour, Acta Crystallogr., Sect. B: Struct. Sci. **47**, 935 (1991).

[41] J.M. Ginder and A.J. Epstein, Phys. Rev. B **41**, 10 674 (1990).

[42] J.H. Simpson, D.M. Rice, and F.E. Karasz, J. Polym. Sci., Part B: Polym. Phys. **30**, 11 (1992).

[43] B. Toudic, J. Gallier, P. Rivet, and H. Cailleau, Solid State Commun. **47**, 291 (1983).

[44] H.M. Rietveld, E.N. Maslen, and C.J.B. Clews, Acta Crystallogr., Sect. B: Struct. Crystallogr. Cryst. Chem. **26**, 693 (1970).

[45] Y. Delugeard, J. Desuche, and J.L. Baudour, Acta Crystallogr., Sect. B: Struct. Crystallogr. Cryst. Chem. **32**, 702 (1976).

[46] J.L. Baudour, H. Cailleau, and W.B. Yelon, Acta Crystallogr., Sect. B: Struct. Crystallogr. Cryst. Chem. **33**, 1773 (1977).

[47] D.D.C. Bradley, J. Phys. D **20**, 1389 (1987).

[48] C.J. Finder, M.G. Newton, and N.L. Allinger, Acta Cryst. B **30**, 411 (1974).